The Influence of the Deposition Parameters on the Properties of Ni-Cu Deposition

OANA CLAUDIA CIOBOTEA BARBU[1,2], IOANA ALINA CIOBOTARU[1]*, FLORIN MIHAI BENGA[1], DANUT IONEL VAIREANU[1]

[1]University Politehnica of Bucharest, Faculty of Applied Chemistry and Materials Science, 1-7 Polizu Str., 011061, Bucharest, Romania

[2]Geological Institute of Romania, 1 Caransebes Str., 01227, Bucharest, Romania

This paper discusses the properties of some Ni-Cu deposits obtained on a steel substrate, which may be employed as supercapacitor plates. In order to achieve plates with different properties, one has varied the parameters of the deposition process such as deposition time, current density and temperature. Scanning electron microscopy and dispersive energy spectrometry were employed for the determination of the structure and composition of the Ni-Cu deposits. The plates with the Ni-Cu deposits were used to create supercapacitors and their capacitance values were also determined.

Keywords: Ni-Cu deposits, scanning electron microscopy, capacitance measurements

Supercapacitors, also known as electrochemical capacitors or ultracapacitors, have been studied for more than 50 years. They are considered to be a potential application for energy storage in order to replace the conventional batteries [1-4]. One of the characteristics of the supercapacitors is that they can store a much higher amount of energy than the conventional capacitors. Generally, a supercapacitor consists of two electrode plates, the most employed electrodes being the porous ones, a dielectric separator and an electrolyte [5].

High dimensions and high surface area of the nanostructure provide easy diffusion paths and improved diffusivity, essential for supercapacitors in order to increase their performance, while low proportions offer good mechanical stability. Morphology plays an important role in defining the performance of an electrode [6], the two above mentioned properties being achieved by means of a foam deposition [7].

Significant progresses have been made in the last century regarding the supercapacitor plates reinforcement research. It consists of various materials such as polymers, metals, ceramics and glass [2]. A large number of supercapacitors have carbon-based reinforcement due to their high performance and high power density [8]. Research studies have been carried out on copper oxide obtained by chemical deposition [9], copper-based reinforcements deposited on steel in ionic liquids [10], nickel oxides reinforcements also obtained by chemical deposition [11] or sol-gel or electrostatic sputter deposition [1].

The properties of these deposits can be controlled by adjusting the working parameters such as deposition time, applied current density, chemical composition of electrolyte, temperature, etc. [12-14].

The aim of this paper is to characterize some Ni-Cu foams deposited on steel substrates that may be employed as supercapacitor plates. The structural characterization of the Ni-Cu foams was performed by scanning electron microscopy, dispersive energy spectrometry and the properties of the supercapacitors obtained were determined by measuring their capacitance.

Experimental part
Materials and methods

The deposition solution consists in a mixture of 0.5M $CuSO_4 \cdot 5H_2O$ (Sigma-Aldrich), 0.01M $NiSO_4 \cdot 7H_2O$ (Sigma-Aldrich), 1.5M H_2SO_4 (Chim Reactiv), 1M HCl (Chim Reactiv) [4].

The electrochemical deposition cell consists of a steel plate electrode (1.6 cm²) used as cathode, a platinum mesh (6 cm²) used as anode and the above mentioned electrolyte solution. The steel plates used as substrate for the Ni-Cu deposits were polished with coarse (600) and fine emery paper (2000), cleaned and rinsed with distilled water and ethylic alcohol. After the cleaning process, the steel plate was dried and insulated on one side so that the deposition of the layers is performed only on one side.

In order to characterize the Ni-Cu deposits, one has investigated some Ni-Cu layers deposited on a steel substrate in different working conditions. The parameters varied during deposition are the current density (1.3A/cm² and 0.9A/cm²), temperature (20 and 40°C) and deposition time (125 and 75 s).

In order to deposit at a constant value of the temperature, one has used a thermostated water bath fitted with a precision thermometer 20°C and, respectively, 40°C. After the deposition of the layers, the plates were dried at 180 ± 5^0C in an oven for one hour.

For the capacitance measurements, one has used as a dielectric separator and a solid ionic electrolyte (a Nafion 117® membrane, DuPont).

Scanning electron microscopy (SEM) was employed in order to determine the morphology and structure of the deposition crystals.

Energy Dispersive Spectrometry (EDS) was employed in order to determine the composition of the deposited layers [15].

The analyses were performed with a ZEISS Merlin Gemini II scanning microscope with a resolution of 0.9 nm. The detector used for the quantitative and semi-quantitative analyses is an EDS OXFORD Instruments X-Max 50 detector. The microscope is equipped with an electron gun, Schottky source, works at high vacuum and has a power up to 1 000 000 X.

In order to measure the capacitance, one has constructed a supercapacitor from two plates with the Ni-Cu layers deposited in identical conditions and separated by a Nafion 117® membrane as dielectric separator. The value of the capacitance was measured using a LCR-Multimeter 4095.

* email: ioanaalinaciobotaru@yahoo.com

Results and discussions

a)The structure of the Ni-Cu deposits

The structure of the Ni-Cu deposits was investigated using the scanning electron microscopy. The images recorded with the microscope were at magnifications situated in the range of 40x and 14kx to identify the formation and shape of the crystals. Ni-Cu deposits with different morphologies were obtained by varying the deposition working parameters.

In figures 1 and 2 are represented the electronic images of the Ni-Cu deposits obtained at a current density of 1.3A/cm² for 125 seconds at 20°C (fig. 1.) and at 40°C (fig. 2.). One may see that the deposit obtained at 20°C has a higher pore density than the one obtained at 40°C. Also one may see, that at a low deposition temperature, the deposited layer is more compact and free from cracks than the one deposited at a higher temperature.

In figures 3 and 4 are shown the electronic images of Ni-Cu deposits obtained at a current density of 1.3A/cm² for 75 s at 20°C (fig. 3.) and at 40°C (fig. 4.). One may see

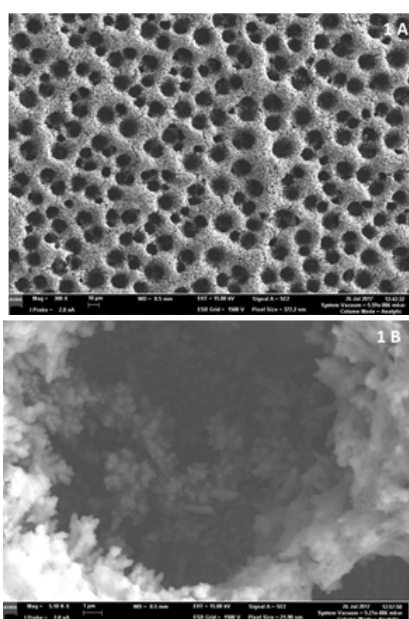Fig. 1. SEM images of Ni-Cu deposits obtained at a current density of 1.3A/cm² for 125 seconds at 20°C, magnification 300x (a.) and 5000x (b.)
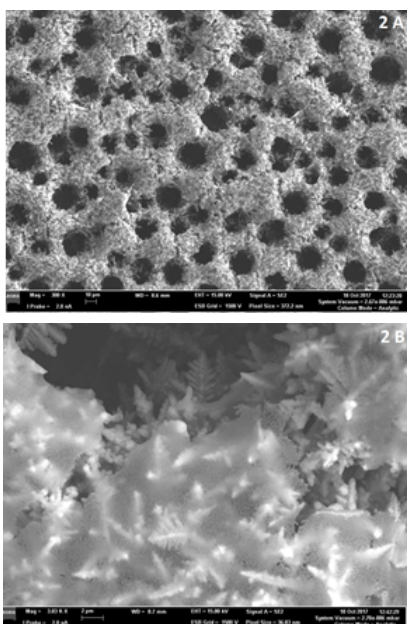

Fig. 2. SEM images of Ni-Cu deposits obtained at a current density of 1.3A/cm² for 125 s at 40°C, magnification 300x (a.) and 3000x (b.)
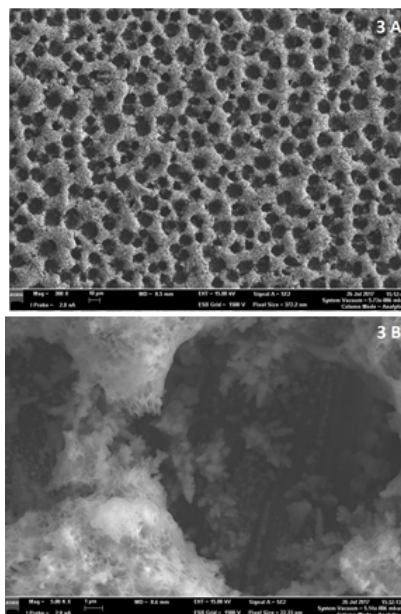

Fig. 3. SEM images of Ni-Cu deposits obtained at a current density of 1.3A/cm² for 75 sat 20°C, magnification 300x (a.) and 5000x (b.)
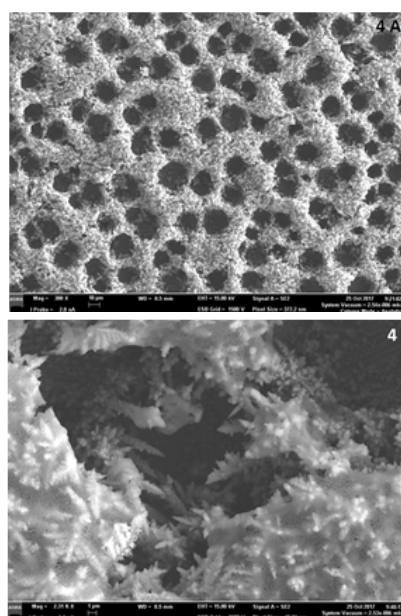

Fig. 4. SEM images of Ni-Cu deposits obtained at a current density of 1.3A/cm² for 75 seconds at 40°C, magnification 300x (a.) and 2000x (b.)

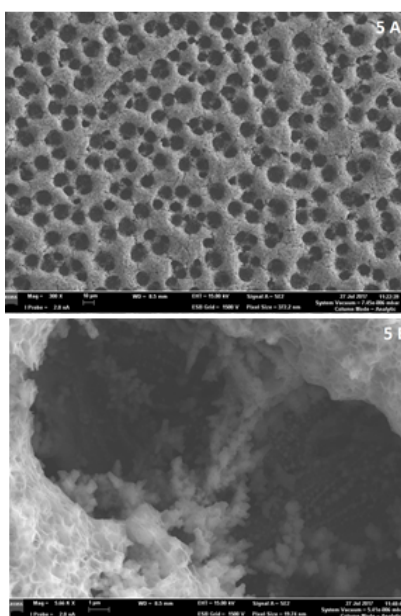Fig. 5. SEM images of Ni-Cu deposits obtained at a current density of 0.9A/cm² for 125 s at 20°C, magnification 300x (a.) and 5000x (b.)

that, as in the previous case, the deposit obtained at 20°C has a higher pore density than the one obtained at 40°C, but the layer deposited at 40°C is thicker than the one achieved at 20°C.

The SEM images of the Ni-Cu deposits obtained at a current density of 0.9 A/cm² for 125 s at 20°C and 40°C are shown in figures 5 and, respectively 6. One may see that the deposit obtained at 20°C has a higher pore density than
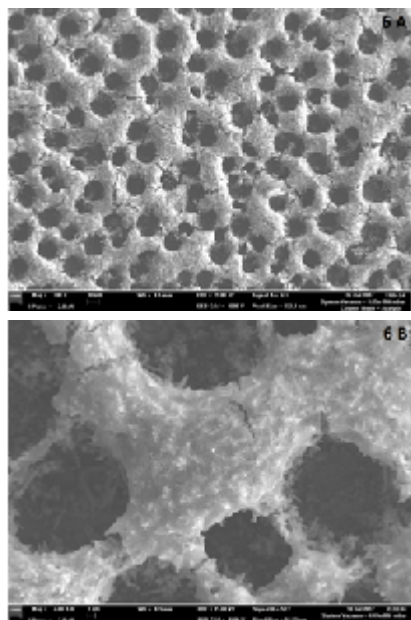
Fig. 6. SEM images of Ni-Cu deposits obtained at a current density of 0.9A/cm² for 125 seconds at 40ºC, magnification 300x (a.) and 2000x (b.)
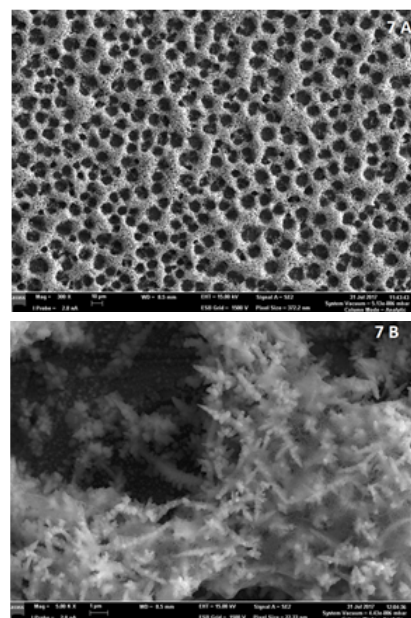

Fig. 7. SEM images of Ni-Cu deposits obtained at a current density of 0.9A/cm² for 75 seconds at 20ºC, magnification 300x (a.) and 5000x (b.)

Fig. 8. SEM images of Ni-Cu deposits obtained at a current density of 0.9A/cm² for 75 s at 40ºC, magnification 300x (a.) and 2000x (b.)

a higher pore density than the one obtained at 40ºC. This behavior was noticed for all the tested Ni-Cu samples.

As can be seen from table 1, the average of the pore diameter and the thickness of the bonding bridges are influenced by the parameters of the deposition process. For the depositions performed at a current density of 1.3 A/cm², one may see that the average pore diameter increases from 10 μm to 22 μm, as the deposition time decreases and the temperature increases. The same behaviour is noticed for the layers deposited at a current density of 0.9 A/cm², where the average pore diameter increases from 9 μm to 16 μm, as the deposition time decreases and the temperature increases.

The average thickness of the bridge may be controlled from the parameters of the deposition process because its dimension is strongly influenced by the variation of the deposition parameters (current density, deposition time and temperature). For example, the deposits obtained at 40ºC and at a current density of 1.3 A/cm² are thicker, increasing the bonding bridges. The sample deposited for 125 seconds has an average thickness of 34 μm and the one deposited for 75 s showed an average thickness of 16 μm.

One may see that the average thickness of bridges increases by increasing the temperature and the time of the deposition process.

b)The composition of the Ni-Cu deposits
The composition of the deposited layers was performed by energy dispersive spectrometry (EDS) using an electron microscope. In table 2, one may see the percent of the main components of interest (Cu and Ni), the remaining

the one obtained at 40ºC. Another feature of both layers (deposited at 20 and 40ºC) is that they are thinner than the ones obtained at a higher current density (1.3 A/cm²), but at the same deposition time (125 s).

In figures 7 and 8 are represented the electronic images of the Ni-Cu deposits obtained at a current density of 0.9A/cm² for 75 s at 20ºC (fig. 7.) and at 40ºC (fig. 8.). One may see that these layers of Ni-Cu deposit are the thinnest deposits obtained. Also, at the layer deposited at 20ºC has
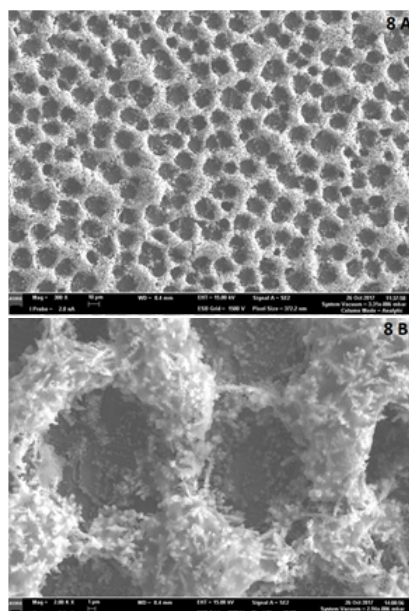
Deposition parameters		Temperature, ºC			
		20ºC		40ºC	
Current density, A/cm²	Time, s	Average pore diameter, μm	Average bridge thickness, μm	Average pore diameter, μm	Average bridge thickness, μm
1.3	125	10	20	19	34
1.3	75	10	10	22	16
0.9	125	9	12	16	22
0.9	75	11	9	15	11

Table 1
THE AVERAGE VALUES OF THE DIAMETER AND THICKNESS OF BRIDGES FORMED IN THE LAYERS

Deposition parameters		Composition, % (20°C)		Composition, % (40°C)	
Current density, A/cm²	Time, s	Cu	Ni	Cu	Ni
1.3	125	42.34	14.85	46.81	14.47
1.3	75	44.18	14.22	47.55	17.28
0.9	125	48.15	10.61	39.09	4.64
0.9	75	52.62	10.52	49.30	15.89

Table 2
THE Ni-Cu PUNCTUAL COMPOSITION IN THE TESTED LAYERS

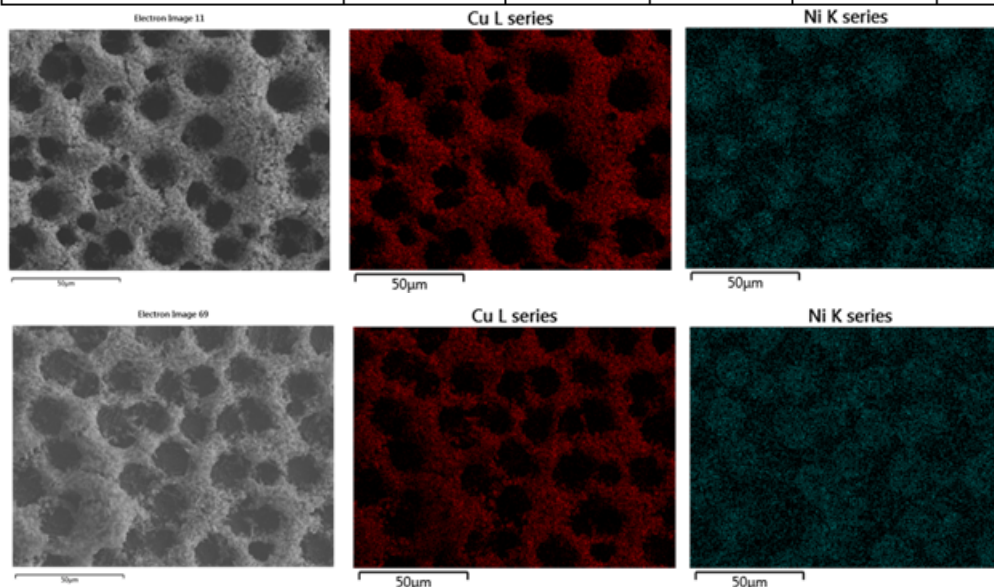
Fig. 9. The element distribution map of the Ni-Cu deposit obtained at a current density of 1.3 A/cm² for 125 s at 20°C, magnification 800x

Fig. 10. The element distribution map of the Ni-Cu deposit obtained at a current density of 0.9 A/cm² for 75 s at 40°C, magnification of 800x

Deposition parameters		Capacitance, µF	
Current density, A/cm²	Time, s	20°C	40°C
1.3	125	29.03	62.7
1.3	75	36.03	27.6
0.9	125	17.8	5.7
0.9	75	41	19.6

Table 3
THE VALUES OF THE CAPACITANCE

percent up to 100% consisting of iron, carbon, oxygen, chlorine and sulphur in various percentages. It can be noticed that by varying the deposition parameters such as current density, time and temperature it is possible to achieve layers with different Ni and Cu content.

From table 2, one may see that by decreasing the current density and the deposition time, the concentration of Cu increases up to 52.62% (at 20°C) and up to 49.30% (at 40°C). Also, for the layers deposited at 20°C and at the same current density, one may see that the concentration of Ni shows a very small decrease with decreasing the time of deposition.

c) Distribution map

In order to determine the distribution of Cu and Ni in the deposited layers, one has recorded the element distribution maps. One may see that the element distribution is not influenced by the variation of the deposition process and that even though one may vary the current density or the deposition time, the nickel concentration is higher near the steel substrate than the one at the surface, where the concentration of copper is higher near the surface. In figures 9 and 10, the distribution maps of Cu (red) and Ni (turquoise) elements are shown.

d) Capacitance measurements

The values of the recorded capacitance for the tested supercapacitors are presented in table 3.

From table 3, one may see that at a deposition temperature of 20°C, with the decrease of the current density and the deposition time, when Ni concentration decreases and Cu increases, an increase in the capacitance value up to 41µF is noticed. For the deposition performed at 40°C, Cu concentration increases, as does Ni, leading to a decrease of the capacitance value, for the layers deposited at 1.3A/cm², and to an increase of the capacitance for the layers deposited at a current density of 0.9 A/cm².

Conclusions

This paper shows the influence of the deposition parameters on the properties of the Ni-Cu deposits. One may see that by varying the current density, the time of the deposition and the temperature of the solution during the deposition, layers of Ni-Cu with different properties are achieved. For example, increasing the current density and the deposition time, one may see that the thickness of the deposited layer is increased.

By varying the deposition parameters n, one may obtain different layers compositions, e.g. for the layers deposited at 20°C, decreasing the current density and deposition time, the Ni concentration decreases from 14.85 to 10.52%.

The Ni-Cu layers deposited have a porous structure with sizes in the range of 9 and 22 μm, depending on the employed parameters during the deposition process.

References

1. LOKHANDE, C.D., DUBAL, D.P., OH-JOO, Curr. Appl. Phys., **11**, 2011, p. 255-270.
2. DEVIVIER, C., TAGLIAFERRI V., FROVALUSCI, F., UCCIARDELLO, N., Mater. Des., **85**, 2015, p. 272-278.
3. MIRZAEIAN, M., OGWU, A.A., JIRANDEHI, H.F., AIDAROVA, S., OSPANOVA, Z., TSENDZUGHUL, N., Colloids Surf. A, **519**, 2017, p. 223-230.
4. EUGENIO S., SILVA T. M., CARMEZIM M. J., DUARTE R. G., MONTEMOR M. F., J. Appl. Electrochem., **44**, 2014, p. 455–465.
5. RADUCAN E., Stocarea energiei electrice folosind noi dispozitive capacitive, PhD thesis summary, 2001, Galati, available on-line at https://www.arthra.ugal.ro:8443/bitstream/handle/123456789/2837/Rezumat_Teza_Raducan_Elena_2011.pdf?sequence=1&isAllowed=y
6. DAR, F.I., MOONOOSWAMY, K.R., ES-SOUNI, M., Nanoscale Res. Lett., **8/363**, 2013, p.1-7.
7. TAPPAN, B.C., STEINER, S.A., LUTHER E.P, Nanoporous metal foams. Angew Chem Int Ed., **49**, no. 27, 2010, p. 4544–4565.
8. WU, N., LOW, J., LIU, T., YU, J., CAO, S., Appl. Surf. Sci., **413**, 2017, p. 35-40.
9. DUBAL, D.P., DHAWALE, D.S., SALUNKHE, R.R., JAMDADE, V.S., LOKHANDE, C.D., J. Alloys Compd, **492**, 2010, p. 26-30.
10. POPESCU, A.M.J., CONSTANTIN, V., OLTEANU, M., DEMIDENKO, O., YANUSHKEVICH, K., Rev. Chim. (Bucharest), **62**, no. 6, 2011, p. 627-632.
11. PATIL, U.M., SALUNKHE, R.R., GURAV, K.V., LOKHANDE, C.D., Appl. Surf. Sci., **255**, 2008, p. 2603-2607.
12. GORANOVA, D., AVDEEV, G., RASHKOV, R., Surf. Coat. Technol., **240**, 2014, p. 204-210.
13. PELLICER, E., VAREA, A., PANE, S., SIVARAMAN, K.M., NELSON, B.J., SURINACH, S., BARO, M.D., SORT, J., Surf. Coat. Technol., **205**, 2011, p. 5285-5293.
14. GONZALEZ MERCADO, G.V., GONZALEZ, C.J., OLIVA, M.I., BRUNETTI, V., EIMER G. A., Procedia Mater. Sci., **8**, 2015, p. 635-640.
15. NOVAC, R.I, SANDU A.V., VASILESCU, E., SANDU, I., Rev. Chim. (Bucharest), **65**, no. 11, 2014, p. 1306-1309.